Attribution of River-Sourced Floating Plastic in the South Atlantic Ocean Using Bayesian Inference

Claudio Pierard[1], Deborah Bassotto[1], Florian Meirer[2], Erik van Sebille[1]

[1]Utrecht University, Institute for Marine and Atmospheric Research, Princetonplein 5, 3584 CC Utrecht, Netherlands

[2]Utrecht University, Debye Institute for Nanomaterials Science, Inorganic Chemistry and Catalysis, Universiteitsweg 99, 3584 CG Utrecht, Netherlands

Key Points:

- We developed a probabilistic framework to attribute the sources of floating oceanic plastic
- The framework uses Bayes theorem to combine river plastic emissions with Lagrangian simulations
- The framework yields probability maps and age distributions of the most likely source in the region

Corresponding author: Claudio Pierard, `c.m.pierard@uu.nl`

Abstract

Most marine plastic pollution originates on land. However, once plastic is at sea, it is difficult to determine its origin. Here we present a Bayesian inference framework to compute the probability that a piece of plastic found at sea came from a particular source. This framework combines information about plastic emitted by rivers with a Lagrangian simulation, and yields maps indicating the probability that a particle sampled somewhere in the ocean originates from a particular source. We applied the framework to the South Atlantic Ocean, focusing on floating river-sourced plastic. We computed the probability as a function of the particle age, at three locations, showing how probabilities vary according to the location and age. We computed the source probability of beached particles, showing that plastic found at a given latitude is most likely to come from the closest source. This framework lays the basis for source attribution of marine plastic.

Plain Language Summary

Plastic is commonly found floating near the surface of the ocean but it is difficult to know where it was introduced into the environment. For some large plastic items, the origin can be estimated by analysing the information printed on them, but for small particles, this information is typically missing. To estimate the origin of particles at sea, we built a framework that assigns a probability indicating the chance of finding a particle that came from a particular source, found at a specific location of the ocean. The framework uses estimates of plastic emitted by rivers, in combination with a simulation of the transport of particles at the ocean surface, to compute the probability that a particle, found at a particular location in the South Atlantic, comes from a certain river. Similarly, we computed the probability that a particle of a certain age (defined as the time it has been drifting in the ocean) comes from a particular river, showing that the probability changes according to the particle age. Finally, we computed the probability for particles stranded at the coasts of South America and Africa, showing that plastic found on beaches is most likely to come from the closest river.

1 Introduction

Floating plastic items have been found in all of the world's oceans (Eriksen et al., 2014; Van Sebille et al., 2015), but the origins (i.e. where and when the plastic entered the ocean) of these plastic items are often not obvious. For some of the larger macroplas-

tics, the origin can be attributed by careful analysis of labels (e.g. Lebreton et al. (2018);
Schofield et al. (2020); Turner et al. (2021)), but most (micro)plastic particles are too
small and nondescript for their origin to be identified this way. Nevertheless, it is important to assess and possibly attribute the likely source for these smaller particles too,
as they are among the most harmful to marine ecosystems (Koelmans et al., 2019).

Here, we use numerical simulations to compute the pathways of virtual plastic particles that float on the surface of the ocean (Hardesty et al., 2017; Van Sebille et al., 2018).
By tracking particles, it is in principle possible to connect any source with any location.
However, the multitude of possible sources very quickly makes this a computationally
unwieldy approach. To overcome this computational challenge, we here propose using
a Bayesian inference approach to attribute sources in a probabilistic sense.

Such a probabilistic approach has been used before to locate objects lost at sea,
like the submarine Scorpio (Richardson et al., 1971) and the (yet to be found) Malaysian
Airlines flight MH370 (Davey et al., 2016). The main difference between these search &
rescue applications of Bayesian inference and our application in the source attribution
of floating plastic is that the sources of plastic are spatially very heterogeneous, and so
is its distribution at sea.

To develop this probabilistic framework for attribution of likely plastic sources, we
here focus on plastic emitted by rivers, as rivers are considered the principal pathway
for mismanaged plastic waste (MPW) into the ocean (Lebreton & Andrady, 2019). We
selected the South Atlantic Ocean as the study location because the South Atlantic Subtropical Gyre is an accumulation zone for plastic (Cózar et al., 2014; Ryan, 2014; Morris, 1980), but also because of the presence of large urban centers along the American
and African coast that contribute to the plastic found at sea (Jambeck et al., 2018; do
Sul & Costa, 2007), and because we plan to compare our results with samples collected
during a 2019 expedition to the region.

2 Theory

Bayesian inference uses Bayes' Theorem to estimate the conditional probability of
an event happening under certain conditions by combining prior knowledge about the
problem with data obtained through an experiment. In particular, our objective is to
estimate the probability that a particle sampled at sea would come from a certain source.

77   This can be written as the conditional probability $p(R_i|S_{loc})$: the probability of sampling

78   a particle at a location S_{loc} from a specific source R_i.

79   Bayes' theorem offers a way of estimating $p(R_i|S_{loc})$, by combining prior knowl-

80   edge with new observations. In our case, Bayes' theorem is

$$p(R_i|S_{loc}) = \frac{p(S_{loc}|R_i)p(R_i)}{p(S_{loc})}, \tag{1}$$

81   where $p(R_i|S_{loc})$ is the conditional probability that we aim to estimate, $p(S_{loc}|R_i)$ is the

82   opposite conditional probability that can be estimated by performing a numerical sim-

83   ulation (see below), $p(R_i)$ is the probability of a particle being released at a particular

84   source and $p(S_{loc})$ is the probability of sampling a plastic particle in a specific location,

85   regardless of the source. It is important to note that $p(R_i|S_{loc}) \neq p(S_{loc}|R_i)$. The lat-

86   ter term namely indicates the probability of a plastic particle found at a location to come

87   from a specific source, and the former indicates the probability of a particle coming from

88   a specific source being at a location. Each term is commonly referred to by it's inter-

89   pretation. For instance, $p(R_i)$ is denoted as 'the prior' because it represents the prior

90   knowledge of the problem, $p(S_{loc}|R_i)$ is 'the likelihood', which updates our prior knowl-

91   edge from the problem, $p(S_{loc})$ is the 'normalizing constant', and $p(R_i|S_{loc})$ is 'the pos-

92   terior'.

93   In eq. (1), computing the normalizing constant $p(S_{loc})$ requires observations for all

94   plastics in the ocean regardless of their source, which means that $p(S_{loc})$ also considers

95   plastic that comes from sources that are not taken into account in the numerator of eq. (1).

96   Therefore, the posterior probabilities at each S_{loc} would not add to one in each location

97   but instead will add to a fraction that corresponds only to the sources of plastic consid-

98   ered in the study. This is inconvenient when the focus is only on plastic coming from spe-

99   cific sources such as riverine plastic. To overcome this inconvenience, we can constrain

100   the sum of all posterior probabilities to be equal to one

$$\sum_{i=1}^{N} p(R_i|S_{loc}) = 1, \tag{2}$$

101   where the sum is defined for the N number of sources. Then, substituting $p(R_i|S_{loc})$ for

102   eq. (1)

$$\sum_{i=1}^{N} \frac{p(S_{loc}|R_i)p(R_i)}{p(S_{loc})} = 1, \tag{3}$$

103   and by factorizing and solving for $p(S_{loc})$

$$p(S_{loc}) = \sum_{i=1}^{N} p(S_{loc}|R_i)p(R_i), \tag{4}$$

104 we obtain a normalizing constant that only considers the sum of all our hypotheses (i.e.

105 products of prior and likelihoods). Finally, by substituting $p(S_{loc})$ in eq. (1) we get

$$p(R_i|S_{loc}) = \frac{p(S_{loc}|R_i)p(R_i)}{\sum_{i=1}^{N} p(S_{loc}|R_i)p(R_i)}, \tag{5}$$

106 which is an alternative form of Bayes' theorem (Carlin & Louis, 2008) that ensures that

107 the sum of all posterior probabilities is one in each location. This last equation is used

108 in this study.

3 Methodology

3.1 Selecting the Sources and Computing the Prior

111 Our prior is based on the annual amount of riverine plastic estimated by Meijer

112 et al. (2021), who used a probability framework combined with geographical data of MPW

113 to estimate the plastic mass emissions of the world rivers into the ocean, at the location

114 of the river mouths. From their global data set, we selected the locations and annual emis-

115 sions for all 1,010 rivers that emit plastic into the South Atlantic. To avoid immediate

116 beaching, we moved the river mouth locations to the center of the closest ocean grid-cell

117 of the model's flow field. When various rivers shared the same closest grid-cell, we summed

118 their emissions. This condensed the number of release locations to 535 (without affect-

119 ing the total amount of plastic released by the rivers in the South Atlantic).

120 We then clustered the rivers in 10 groups that contained the top polluting rivers

121 and their neighboring rivers. These clusters are 2° by 2° square regions centered around

122 ten locations that coincide with important cities or river estuaries. We used the result-

123 ing 283 river mouth locations in these 10 clusters as the release positions for the parti-

124 cles in the simulation. The 10 clusters (Figure 1) account for 87.9% of the riverine plas-

125 tic emissions in the South Atlantic. There are two clusters on the African coast: around

126 the city of Cape Town and on the Congo River estuary. The other eight clusters are on

127 the South American coast: five near the cities of Rio de Janeiro, Porto Alegre, Santos,

128 Salvador, and Recife; and three on the river estuaries of Rio de la Plata, Itajaí and Paraibá.

129 We defined the prior distribution $p(R_i)$ to be the fraction of plastic emitted at each

130 cluster, normalised by the total amount of plastic emitted at the 10 clusters. Our prior

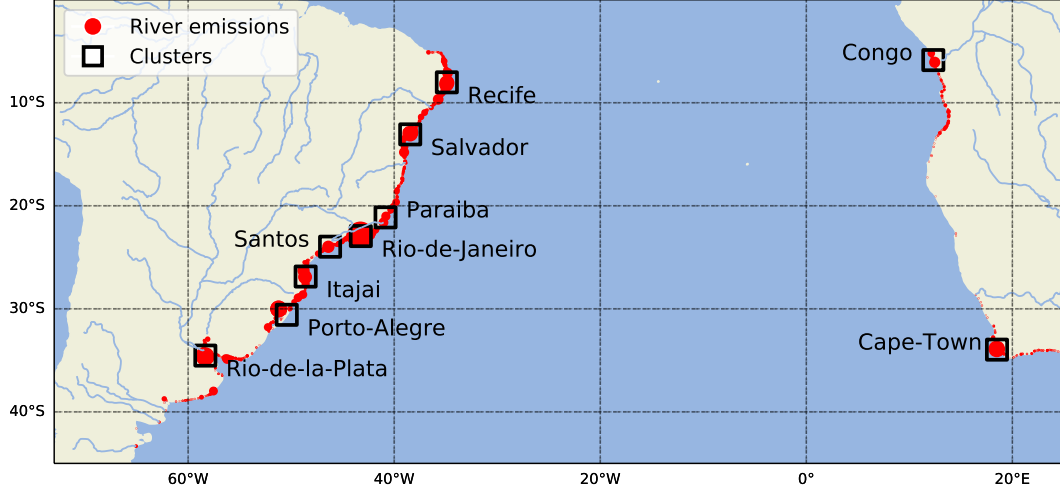131 thus is a 10-dimensional categorical or discrete distribution, in which each source has an

Figure 1. Map of the top 50 rivers (red dots) in the South Atlantic from Meijer et al. (2021) and the clusters (black squares) used as sources in this study. The size of the red circles is proportional to the rivers' plastic emission. The size of the black squares exaggerates the true size of the clusters, which is 2° by 2°.

associated probability defined between 0 to 1, and the sum of the 10 probabilities is 1. The probability associated with each source is shown in Table 1.

3.2 Simulation Setup and Computing the Likelihood

To compute the likelihood $p(S_{loc}|R_i)$, we released virtual particles from each of the sources R_i and tracked them through the South Atlantic surface flow. We performed the simulation using the Parcels framework (Delandmeter & Sebille, 2019) on the Surface and Merged Ocean Currents (SMOC) data set from the Copernicus Marine Environmental Service (CMEMS) (Drillet et al., 2019). The SMOC data set is a 2D surface flow field, with a 1/12° resolution, of the sum of the velocity contributions from the Eulerian component associated with currents, the tidal component, and the Stokes Drift component associated with waves (Drillet et al., 2019). In this study we assumed that the particles were at the surface at all times.

The domain of the simulation was the South Atlantic Ocean, from 70°W to 25°E and between 50°S to the Equator. We used hydrodynamic data from 1 April 2016 to 31 August 2020, releasing particles in the first year only and then tracking them for another 3.4 years. During the simulation, if a particle left the domain, we stopped tracking that

Sources (R_i)	Proportion (%)	$p(R_i)$
Congo	1.6	0.019
Cape Town	4.2	0.051
Rio de la Plata	9.8	0.121
Porto Alegre	8.3	0.099
Santos	4.6	0.048
Paraibá	3.8	0.031
Itajaí	7.5	0.086
Rio de Janeiro	28.5	0.334
Salvador	6.8	0.078
Recife	12.7	0.133
Other rivers	12.1	-

Table 1. The proportion of the total annual plastic released to the South Atlantic and the prior probability $p(R_i)$ of a particle being released at a specific source R_i. The "Other rivers" row indicates the proportion of plastic from rivers outside the clusters and is therefore not considered in $p(R_i)$.

specific particle. We implemented a stochastic parametrization for beaching of buoyant particles as described in Onink et al. (2021), using a beaching timescale of $\lambda_b = 10$ days and a re-suspension timescale of $\lambda_r = 69$ days. To parametrise unresolved turbulence that acts on the floating plastic (Van Sebille et al., 2020), we implemented uniform diffusion defined in the whole domain with a value of $10 \, \text{m}^2 \, \text{s}^{-1}$, similar to Onink et al. (2021) and Lacerda et al. (2019).

We performed one simulation with 100,000 particles per source, with a fourth-order Runge-Kutta integration time step of $1 \, \text{h}$. We released the particles from the 283 river mouth locations inside the 10 clusters. On average, the particles were released $10 \, \text{km}$ from the coast. The number of particles released at each location was proportional to the emission of each of the rivers within the cluster, and equally distributed over one year. We stored the particles' positions every $24 \, \text{h}$, for a total of 1,234 points per trajectory.

We computed the likelihood $p(S_{loc}|R_i)$ by binning the particle positions in $1° \times 1°$ bins. For this, we counted the particles inside each bin at every time step, and then we averaged the number of particles during a time period. Then, we divided the average number of particles at each bin by the sum of all the averaged counts in all bins. The $p(S_{loc}|R_i)$ in each bin has a value between 0 and 1 and the sum of the probabilities of all bins is 1. This yielded 10 $p(S_{loc}|R_i)$ maps, one per source R_i.

The likelihood was computed based on the positions of the particles according to their age. The particle age represents the transit time of particles between the source R_i and a sampling location S_loc (i.e., their drifting time), with each particle following a different pathway until reaching S_{loc} (Van Sebille et al., 2018).

3.3 Oceanic Particles Posterior Probability

We computed the posterior probability $p(R_i|S_{loc})$ using eq. (5) independently for each $1°$ by $1°$ bin, using the corresponding likelihood and the normalizing constant in each particular bin. Doing this for all the sources, we get the local posterior distribution in each bin, as a probability between 0 and 1 for each source. This results in 10 posterior probability maps (one per source) which add up to 1 for each bin.

3.4 Beached Particles Posterior Probability

Since we use a stochastic parametrization for simulating the beaching of particles near the coast, we can also map the probability of a beached particle coming from a specific source. To compute this, we built two cumulative latitudinal histograms of the particles that were beached at a specific time step: one for the American coast and the other for the African coast. The cumulative latitudinal histogram is formed by counting the particles that are beached in latitudinal bins of 1°, disregarding the longitude of those particles, and by classifying them into particles that beached either at the American or the African coast. With the counts per latitude, we computed the average at each bin for the duration of the whole simulation and normalized by the sum of all average counts per bin. As for the posterior probability maps, we computed the beached posterior probability $p(R_i|S_{lat})$ using eq. (5), where S_{lat} is the latitudinal bin.

4 Results

4.1 Likelihood Maps

Figure 2 shows the likelihood maps for particles released at each source R_i, averaged over a period of 3.4 years. The values for the likelihood in the bins are between 0 to 10^{-4}, as they represent the proportion of particles (in relation to the total number of particles from a source in the domain) that cross a grid cell. Each source has 100,000 particles, minus the particles that exited the domain at a certain time step, so if in one bin there are 100 particles, the likelihood would be in the order of 10^{-4}.

In general, the dark blue areas represent regions where almost no particles were found from a specific source, while the yellow regions represent locations where it was more likely to find particles from that source. Specifically, for the South American sources, the likelihood of finding particles from Recife, Santos, and Salvador is almost zero in the open ocean between 20 °S to 40 °S, that is, where the subtropical gyre is located. The particles released from those sources tend to stay close to shore and beach because of the effect of Stokes drift that pushes them towards the coast.

For the sources Itajaí, Paraíba, Porto Alegre, Rio de Janeiro, and Rio de la Plata, the likelihood to find particles released by any of those sources is the highest in the subtropical gyre (between 20 °S to 40 °S), with values ranging from 1×10^{-4} to 3×10^{-4}, suggesting a high chance of finding particles from those sources, with Porto Alegre be-
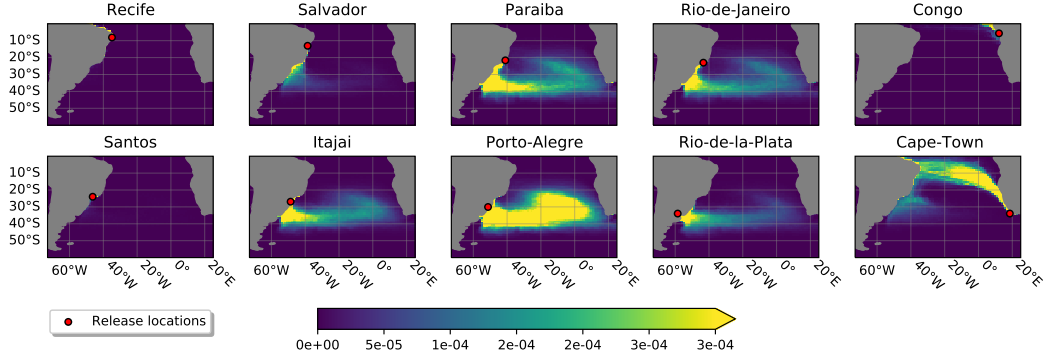
Figure 2. Likelihood maps of the spatially binned $p(S_{loc}|R_i)$ for each source. The color scale indicates the probability of finding a plastic particle coming from the source (indicated as a red point).

ing the largest contributor. Closer to the South American coast, the likelihood is above 3×10^{-4} for all these sources. North of the gyre, from 20°S and further north, the likelihood of finding particles from the American coast is near-zero.

For the African sources, shown on the right of Figure 2, we see that the likelihood of finding particles released in Cape Town is the highest in the Benguela Current. These particles are likely to reach the South American coast near the Cape of Saõ Roque, and will less likely get carried by the Brazil Current towards the coast of Argentina. The particles released at the Congo get carried away northward to the Equator, outside of the domain of our simulation, and are unlikely to find these particles in other parts of the studied domain.

4.2 Oceanic Particles Posterior Probability

Figure 3 shows the posterior probability $p(R_i|S_{loc})$ maps for each source, averaged over 3.4 years. In particular, the particles in our simulation did not reach latitudes south of 50°S, leading to no defined posterior probability in the Antarctic Circumpolar Current (ACC). This is due to the generally northward Ekman drift in the ACC (Onink et al., 2019), and because we assumed that the particles only originate from ten sources placed north of 50°S. In total, 130,585 particles exited the domain: 97,926 across the Equator and 32,659 into the Indian Ocean.

Regarding the individual panels in Figure 3, the posterior probabilities for Recife and Santos were near-zero because only very few particles were transported into the open ocean. The probability that particles that end up between 50°W to 40°W and close to Brazil originated from Salvador was up to 30%. The posterior probabilities of Itajaí and Paraíba were below 20% everywhere, with the highest values located in the subtropical gyre, while probabilities were close to zero in the rest of the domain. For Rio de la Plata, the highest probabilities were found at the boundary with the ACC, approaching 40% in probability, with decreasing values when going from there towards the equator. The two sources that dominated in the region of the subtropical gyre, between 20°S to 50°S, were Porto Alegre and Rio de Janeiro, with probabilities around 40%. South of South Africa, particles released from Rio de Janeiro are dominant, contributing 60% to the probability. The remaining 40% are mainly contributed by Porto Alegre and Rio de la Plata. In the Benguela Current region and extending northwest to the northern coast of Brazil, the probability is close to 100% that particles originate from Cape Town. Finally, the posterior probability of Congo is almost only located near the source and farther north.
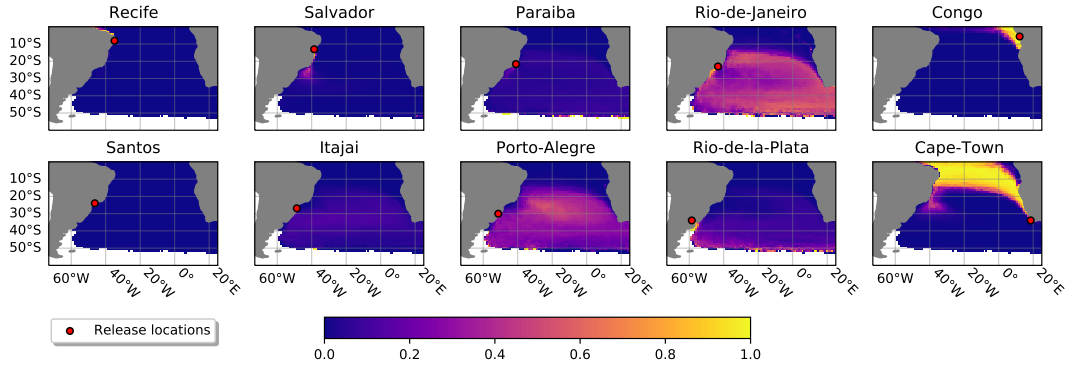

Figure 3. Posterior probability maps, averaged over 3.4 years, showing $p(R_i|S_{loc})$, the probability of finding a particle from a specific source at any point in the South Atlantic. Each map displays the probability for a specific source in all the bins of the domain. The red dots indicate the locations of the sources from which the particles entered the ocean.

4.3 Local Posterior Age Distributions

The posterior age distributions yield the probable sources of a particle of a certain age, sampled at a certain location. Figure 4 shows the posterior age distributions for three sampling locations, averaged over a time window of 30 days. The dashed line represents

the number (N) of particles that reach the location as a function of age. The posterior

probability distributions were only computed when $N > 10$.

The panel for sampling location A in Figure 4, located in the western part of the

subtropical gyre (32.37°S, 37.64°W), shows for example that a particle sampled at that

location with age younger than 0.4 years is very unlikely to come from any of the con-

sidered river sources. For particles between 0.4 years to 1.0 years, the most probable sources

are Salvador and Porto Alegre. For ages older than 1.0 years, the probability from Sal-

vador drops below 20% while Rio de Janeiro grows. For particles older than 1.5 years,

Porto Alegre and Rio de Janeiro have the largest probabilities, with values fluctuating

between 20% and 40%. The rest of the sources have values below 20%.

The posterior age distributions for location B (32.37°S, 5.80°E) in Figure 4, show

that it is unlikely to find particles younger than 1.2 years coming from any of the con-

sidered sources: only particles older than 1.4 years can reach this point. Similar to point

A, the sources with the largest probability, throughout all ages, are Rio de Janeiro and

Porto Alegre. For the younger particles, these probabilities oscillate around 50%, while

for older particles, the two sources decrease down to 30% for 3.4-year-old particles. The

remaining sources stay below 20% for all ages. The plot corresponding to point C located

north of the gyre (19.19°S, 13.39°W), shows that particles reach this location two years

after release. Fewer particles were present on average compared to A and B, reaching

a peak N at 2.7 years. The largest probability corresponds to Rio de Janeiro and Porto

Alegre. Rio de Janeiro is the predominant source of particles of all ages, although, Porto

Alegre becomes significant when particles are 2.5 years old or older. The other sources

remain below 10% for all ages recorded.

4.4 Beached Particles Posterior Probability

Figure 5 shows the posterior probabilities for a particle to beach at certain latitude,

$p(R_i|S_{lat})$, based on its origin. The $p(R_i|S_{lat})$ for the American coast are displayed in

the right panel and the ones for the African coast are shown in the left panel. On the

American coast, the nearest source to the bin S_{lat} has the highest probability, which peaks

at the same latitude as the source or in its vicinity. This suggests that the plastic found

on beaches close to a source is most likely to come from that source. Santos is the only

exception to this trend because its probability is overshadowed by its proximity to Rio de Janeiro which emissions are six times larger.

In the right panel of Figure 5, the beached probabilities for latitudes between 25°S to 35°S on the African coastline show a dominance of particles coming from the American coast, accounting for 90% of the beached particles. The probability of the beached particles coming from Cape Town was found to be less than 10% in this region. Between 18°S to 25°S, Cape town was the only source for beached particles. There were also regions, namely between 12°S to 14°S and 16°S to 18°S, where no particles of any of the considered sources beached. Finally, at latitudes between 5°S to 12°S, the only probable source was Congo, no particles from other sources beached that far north. The reason that we found 100% probability for one single source or no beached particles at all, is that we only considered two sources in Africa, which were at the borders of the studied domain. In the future, more sources need to be considered, both in this region and outside, to improve these estimates.

5 Conclusions and Discussion

We introduced a Bayesian probabilistic framework that allowed us to estimate $p(R_i|S_{loc})$, the probability that a plastic particle, sampled at the surface of the South Atlantic Ocean, came from a particular source. The framework supports different types of analyses and can be used, for example, to compute spatial probabilities, compute local probability as a function of particle age, or analyse the probabilities once a physical process (such as beaching) alters the particles' state.

The time average window used for computing the likelihood $p(S_{loc}|R_i)$ can be adjusted according to the aim of the study. Usually, computing the likelihood for small time windows leads to greater variability in the likelihood and for instance in the posterior probability. For these reasons, we computed the average likelihood on the whole simulation and from there we computed the posterior probability.

As we showed in Figure 3, visualizing the posterior $p(R_i|S_{loc})$ in maps allows us to identify the most important sources that pollute ocean regions that provide high ecosystem services and that are vulnerable to plastic, such as subtropical gyres (Helm, 2021) and marine protected areas (Krüger et al., 2017). This can be used to prioritize the reduction of MPW in the principal sources to mitigate the problem. In particular, Porto

Alegre and Rio de Janeiro are the most probable sources of riverine plastic in the South Atlantic Subtropical Gyre.

The local posterior age distributions, shown in Figure 4 further illustrate the analysis that can be done by selecting a location and by computing the probability distributions as a function of the particle's age. This can point us to the most likely source if we estimate the time the plastic has been drifting in the ocean, by assessing its degradation (Chamas et al., 2020; Gewert et al., 2015).

The latitudinal beached posterior probabilities, shown in Figure 5, demonstrate how this framework can be used to analyse the contribution of different sources to particle sinks (such as beaches) when considering certain physical processes that alter particle pathways (such as the process of beaching). This can be expanded to including other additional physical processes that can alter the dynamical state of the virtual particles, such as sinking (Lobelle et al., 2021).

This study focuses on floating plastic coming from rivers that discharge plastic into the South Atlantic. In our analysis, we ignore plastic entering the domain from the Indian Ocean leakage (Van der Mheen et al., 2019) and from the North Atlantic (Speich et al., 2007). To consider it, we need to assume these leakages as sources, by knowing how much plastic enters the domain through the boundaries, or expand the domain to consider other basins.

One major advantage of the Bayesian nature of our framework is that it allows updating the results when better estimates of plastic emissions are available without having to redo the (computationally expensive) Lagrangian simulations. For instance, it can be expanded by including a prior that accounts for seasonal variations in river-borne plastic inputs, or by taking into account different types of land-based or sea-based sources.

The output data from the simulations is available through `https://doi.org/10` `.24416/UU01-90F027`. The supporting figures, tables, and text can be found in the supporting information file associated with this article.

References

Carlin, B. P., & Louis, T. A. (2008). *Bayesian methods for data analysis.* CRC Press.

Chamas, A., Moon, H., Zheng, J., Qiu, Y., Tabassum, T., Jang, J. H., . . . Suh, S. (2020). Degradation rates of plastics in the environment. *ACS Sustainable Chemistry & Engineering*, *8*(9), 3494–3511.

Cózar, A., Echevarría, F., González-Gordillo, J. I., Irigoien, X., Úbeda, B., Hernández-León, S., . . . others (2014). Plastic debris in the open ocean. *Proceedings of the National Academy of Sciences*, *111*(28), 10239–10244.

Davey, S., Gordon, N., Holland, I., Rutten, M., & Williams, J. (2016). *Bayesian methods in the search for mh370.* Springer Nature.

Delandmeter, P., & Sebille, E. v. (2019). The parcels v2. 0 lagrangian framework: new field interpolation schemes. *Geoscientific Model Development*, *12*(8), 3571–3584.

do Sul, J. A. I., & Costa, M. F. (2007). Marine debris review for latin america and the wider caribbean region: from the 1970s until now, and where do we go from here? *Marine Pollution Bulletin*, *54*(8), 1087–1104.

Drillet, Y., Chune, S. L., Levier, B., & Drevillon, M. (2019). Smoc: a new global surface current product containing the effect of the ocean general circulation, waves and tides. In *Geophysical research abstracts* (Vol. 21).

Eriksen, M., Lebreton, L. C., Carson, H. S., Thiel, M., Moore, C. J., Borerro, J. C., . . . Reisser, J. (2014). Plastic pollution in the world's oceans: more than 5 trillion plastic pieces weighing over 250,000 tons afloat at sea. *PloS one*, *9*(12), e111913.

Gewert, B., Plassmann, M. M., & MacLeod, M. (2015). Pathways for degradation of plastic polymers floating in the marine environment. *Environmental science: processes & impacts*, *17*(9), 1513–1521.

Hardesty, B. D., Harari, J., Isobe, A., Lebreton, L., Maximenko, N., Potemra, J., . . . Wilcox, C. (2017). Using numerical model simulations to improve the

understanding of micro-plastic distribution and pathways in the marine environment. *Frontiers in marine science*, *4*, 30.

Helm, R. R. (2021). The mysterious ecosystem at the ocean's surface. *PLoS Biology*, *19*(4), e3001046.

Jambeck, J., Hardesty, B. D., Brooks, A. L., Friend, T., Teleki, K., Fabres, J., ... others (2018). Challenges and emerging solutions to the land-based plastic waste issue in africa. *Marine Policy*, *96*, 256–263.

Koelmans, B., Pahl, S., Backhaus, T., Bessa, F., van Calster, G., Contzen, N., ... others (2019). *A scientific perspective on microplastics in nature and society*. SAPEA.

Krüger, L., Ramos, J., Xavier, J., Grémillet, D., González-Solís, J., Kolbeinsson, Y., ... others (2017). Identification of candidate pelagic marine protected areas through a seabird seasonal-, multispecific-and extinction risk-based approach. *Animal Conservation*, *20*(5), 409–424.

Lacerda, A. L. d. F., Rodrigues, L. d. S., Van Sebille, E., Rodrigues, F. L., Ribeiro, L., Secchi, E. R., ... Proietti, M. C. (2019). Plastics in sea surface waters around the antarctic peninsula. *Scientific reports*, *9*(1), 1–12.

Lebreton, L., & Andrady, A. (2019). Future scenarios of global plastic waste generation and disposal. *Palgrave Communications*, *5*(1), 1–11.

Lebreton, L., Slat, B., Ferrari, F., Sainte-Rose, B., Aitken, J., Marthouse, R., ... others (2018). Evidence that the great pacific garbage patch is rapidly accumulating plastic. *Scientific reports*, *8*(1), 1–15.

Lobelle, D., Kooi, M., Koelmans, A. A., Laufkötter, C., Jongedijk, C. E., Kehl, C., & van Sebille, E. (2021). Global modeled sinking characteristics of biofouled microplastic. *Journal of Geophysical Research: Oceans*, *126*(4), e2020JC017098.

Meijer, L. J., van Emmerik, T., van der Ent, R., Schmidt, C., & Lebreton, L. (2021). More than 1000 rivers account for 80% of global riverine plastic emissions into the ocean. *Science Advances*, *7*(18), eaaz5803.

Morris, R. J. (1980). Plastic debris in the surface waters of the south atlantic. *Marine Pollution Bulletin*, *11*(6), 164–166.

Onink, V., Jongedijk, C., Hoffman, M., van Sebille, E., & Laufkötter, C. (2021). Global simulations of marine plastic transport show plastic trapping in coastal

zones. *Environmental Research Letters*.

Onink, V., Wichmann, D., Delandmeter, P., & van Sebille, E. (2019). The role of ekman currents, geostrophy, and stokes drift in the accumulation of floating microplastic. *Journal of Geophysical Research: Oceans*, *124*(3), 1474–1490.

Richardson, H. R., Stone, L. D., et al. (1971). Operations analysis during the underwater search for scorpion. *Naval Research Logistics Quarterly*, *18*(2), 141–157.

Ryan, P. G. (2014). Litter survey detects the south atlantic 'garbage patch'. *Marine Pollution Bulletin*, *79*(1-2), 220–224.

Schofield, J., Wyles, K. J., Doherty, S., Donnelly, A., Jones, J., & Porter, A. (2020). Object narratives as a methodology for mitigating marine plastic pollution: multidisciplinary investigations in galápagos. *Antiquity*, *94*(373), 228–244.

Speich, S., Blanke, B., & Cai, W. (2007). Atlantic meridional overturning circulation and the southern hemisphere supergyre. *Geophysical Research Letters*, *34*(23).

Turner, A., Williams, T., & Pitchford, T. (2021). Transport, weathering and pollution of plastic from container losses at sea: Observations from a spillage of inkjet cartridges in the north atlantic ocean. *Environmental Pollution*, *284*, 117131.

Van der Mheen, M., Pattiaratchi, C., & van Sebille, E. (2019). Role of indian ocean dynamics on accumulation of buoyant debris. *Journal of Geophysical Research: Oceans*, *124*(4), 2571–2590.

Van Sebille, E., Aliani, S., Law, K. L., Maximenko, N., Alsina, J. M., Bagaev, A., . . . others (2020). The physical oceanography of the transport of floating marine debris. *Environmental Research Letters*, *15*(2), 023003.

Van Sebille, E., Griffies, S. M., Abernathey, R., Adams, T. P., Berloff, P., Biastoch, A., . . . others (2018). Lagrangian ocean analysis: Fundamentals and practices. *Ocean Modelling*, *121*, 49–75.

Van Sebille, E., Wilcox, C., Lebreton, L., Maximenko, N., Hardesty, B. D., Van Franeker, J. A., . . . Law, K. L. (2015). A global inventory of small floating plastic debris. *Environmental Research Letters*, *10*(12), 124006.
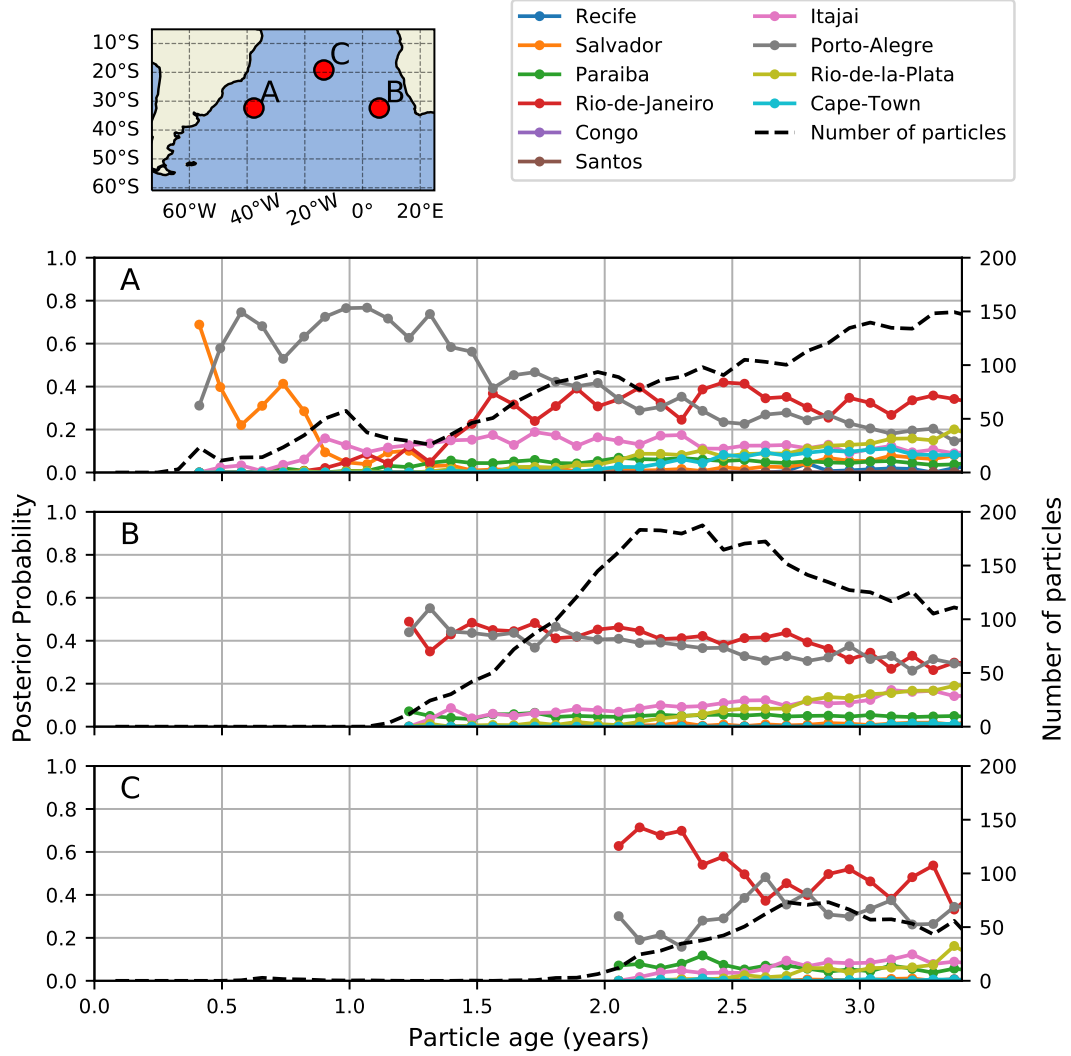
Figure 4. Local posterior age distributions at three different locations for the posterior probability. The map on the top right marks the locations A, B, and C, that correspond to the time series shown in the plots A, B, and C. Each color in A, B and C, represents the probability $p(R_i|S_{loc})$ for a particular source. The black dashed line represents the number of particles (N) at the respective location.
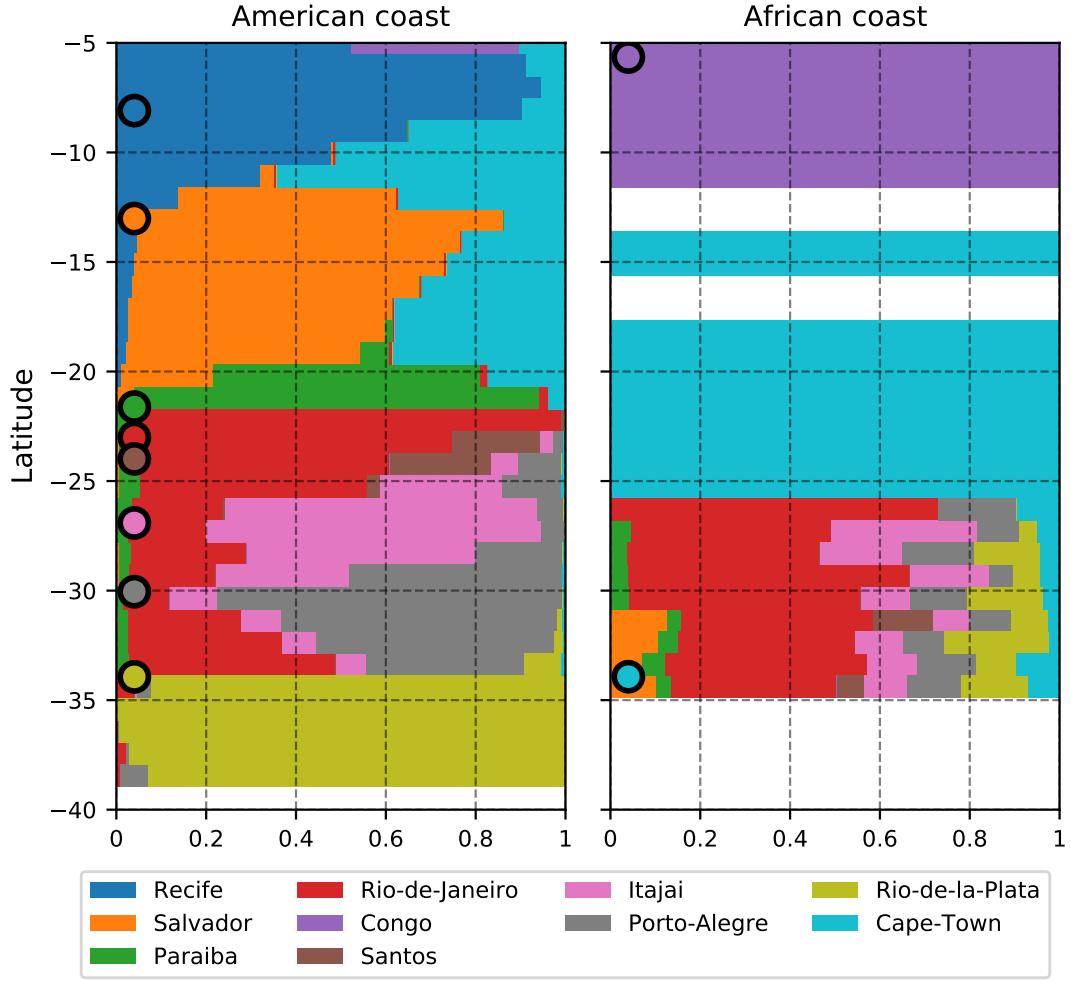
Figure 5. Horizontal bar plot for the posterior probabilities of beached particles (x-axis) at a specific latitude (y-axis). The panel on the left shows the probabilities at the American Coast and the panel on the right the probabilities at the African coasts. Each color is associated with a source, shown in the legend at the bottom. Each latitude has a corresponding horizontal bar summing the probabilities from the sources at that latitude to 1. The round markers on the left of each plot represent the latitudes of the sources. If the marker is on the left panel, the source is at the American coast, and if the marker is in the right panel, the source is located at the African coast.